J Solid State Electrochem (2000) 4: 199–204

ORIGINAL PAPER

Krzysztof Miecznikowski · James A. Cox
Adam Lewera · Pawel J. Kulesza

Solid state voltammetric characterization of iron hexacyanoferrate encapsulated in silica

Received: 8 April 1999 / Accepted: 13 August 1999

Abstract We describe a sol-gel approach by which iron hexacyanoferrate is immobilized in silica in a manner suited to investigation by electrochemistry in the absence of a contacting liquid phase. Such physicochemical parameters as concentration of redox sites (C_o) and apparent (effective) diffusion coefficient (D_{app}) are estimated by performing cyclic voltammetric and potential step experiments in two time regimes, which are characterized by linear and spherical diffusional patterns, respectively. Values of D_{app} and C_o thereby obtained are 2.0×10^{-6} cm^2 s^{-1} and 1.4×10^{-2} mol dm^{-3}. The D_{app} value is larger than expected for a typical solid redox-conducting material. Analogous measurements done in iron(III) hexacyanoferrate(III) solutions of comparable concentrations, 1.0×10^{-2} and 5.0×10^{-3} mol dm^{-3}, yield D_{app} on the level of 5–6×10^{-6} cm^2 s^{-1}. Thus, the dynamics of charge propagation in this sol-gel material is almost as high as in the liquid phase. The residual water in the silica, along with the pore structure, are important to the overall mechanism of charge transport, which apparently is limited by physical diffusion rather than electron self-exchange. Under conditions of a solid state voltammetric experiment which utilizes an ultramicroelectrode, encapsulated iron hexacyanoferrate redox centers seem to be in the dispersed colloidal state rather than in a form of the rigid polymeric film.

Key words Sol-gel chemistry · Silica · Pore structure · Colloidal Prussian Blue · Cyanometallate redox sites

K. Miecznikowski[1] · J.A. Cox (✉)
Department of Chemistry, Miami University,
Oxford, OH 45056, USA

A. Lewera · P.J. Kulesza (✉)
Department of Chemistry, University of Warsaw,
Pasteura 1, PL-02-093 Warsaw, Poland

Permanent address:
[1]Department of Chemistry, University of Warsaw,
Pasteura 1, PL-02-093 Warsaw, Poland

Introduction

Recently, there has been much interest in silica materials prepared by sol-gel processes [1–10]. A feature that is especially important in electrochemical applications is that silica, which is prepared without curing at elevated temperature, has a porous structure that contains water. By introducing high concentrations of surfactants into the sols, the resulting silica is templated into the mesoporous domain [11]. Redox-active substances that are doped in sols are sufficiently mobile to permit study by conventional voltammetric methods, even when the gelation point is reached. An important application is that the voltammetry of ferrocene moieties that were doped into sols provided insight on the chemistry of the sol-gel [1, 7]. Even when the gels are aged, conventional voltammetric methods are useful as long as the working electrode is small enough to produce currents in the nA range. For example, the cyclic voltammetry of heteropolyacids of tungsten that were encapsulated in silica xerogels was similar in terms of peak shapes and positions on the potential axis to those observed in aqueous solution, and when the matrix was templated into the mesoporous range the effective diffusion coefficients approached the values observed in aqueous solution [2, 6]. In these studies, residual water that is present in the pores and on the pore walls has a marked influence on the voltammetry.

The electrochemistry of doped xerogels is a growing area of study because of potential applications as geometrically versatile platforms in such diverse devices as chemical sensors, electrochromic displays, and charge storage systems; moreover, they provide media for fundamental studies of electrocatalysis and charge propagation [3, 11]. Among mixed-valence and ionically conducting polynuclear inorganic systems, Prussian Blue-type metal hexacyanoferrates are of interest as dopants because in other forms, such as films on electrode surfaces, they have been demonstrated to possess the properties that are required for these and

other applications [13–22]. Exploiting these complementary characteristics requires retention both of the attractive properties of these polynuclear compounds when they are dopants in sol-gel materials and of the ability to interrogate the resulting rigid or semi-rigid solids by solid state voltammetry in the absence of liquid electrolyte.

In the present work, iron(III) hexacyanoferrate(III) from the family of Prussian Blue (PB) [13, 20, 23, 24] was investigated as a dopant in silica. In the fabrication procedure, we employed the fact that the oxidized form of PB, i.e. iron(III) hexacyanoferrate(III) or Prussian Yellow, forms homogeneous solutions which are readily doped into the sol. One objective was to determine if the general voltammetric behavior of PB, namely its reversible reduction to Prussian White (Everitt's salt), was retained in the silica. In this regard, the silica provided a transparent matrix with the sizeable population (ionic budget) of counterions that is necessary to provide charge balance during redox reactions. The work was extended to include evaluation of the effective diffusion of iron hexacyanoferrate (FeHCNFe) species in the silica and the concentration of the redox centers in the doped xerogel, because these are important factors in predicting the scope of applications of this material.

Experimental

The solid state electrochemical measurements were performed using a cylindrical cell constructed using the counter electrode as the base and Tygon tubing as the side [2]. The assembly served as a mold into which the sol was added. A glassy carbon disk (diameter, 3 mm) served as the counter electrode. A silver wire that was inserted through the side of the cell served as the reference electrode after coating it with AgCl. The working electrode was a 10-μm dia. carbon fiber disk (Bioanalytical Systems), which was imbedded in the xerogel by mounting it vertically in the mold when the sol was added. Conventional liquid-phase experiments were performed with the carbon fiber working electrode, a Pt-wire counter, and a Ag/AgCl (sat. KCl) reference electrode. Electrodes were polished before use with 0.3-μm alumina with water as the lubricant. All electrochemical experiments were performed with a CH Instruments (Austin, Texas, USA) Model 750 Electrochemical Workstation. The water content in silica was determined from the thermogravimetric analysis measurements which were made with a Perkin Elmer TGA 7 system. All electrochemical measurements and chemical procedures were done at room temperature, 20 ± 2 °C.

Unless otherwise stated, all chemicals were of analytical reagent grade quality and were used without further purification. Tetramethyl orthosilicate (TMOS) of 98% purity was from Aldrich. Triton X-114 (Sigma) was used as surfactant. Solutions were prepared from house-distilled water that was further purified with a Barnstead NANO pure system.

The iron(III) hexacyanoferrate(III) was prepared immediately prior to use from a solution containing 2 mmol dm^{-3} $K_3[Fe(CN)_6]$, 2 mmol dm^{-3} $FeCl_3$, and 0.5 mol dm^{-3} KCl. Unless otherwise noted, the silica sol was formed in a mixture containing 3 cm^3 of TMOS, 3 cm^3 of methanol, 3 cm^3 of 0.1 mol dm^{-3} HCl, and 200 ml of Triton X-114. The solution was stirred for 1 h in a fume hood (note: TMOS is a serious eye hazard; prior to the completion of the gelation, solutions of TMOS must be kept in a fume hood, and protective eyeware must be worn). The doping was accomplished by adding 0.5 cm^3 of the iron(III) hexacyanoferrate(III) solution to the silica sol after the 1-h period and stirring the resulting mixture for an additional 0.5 h. Next, 400 μl of the sol containing iron hexacyanoferrate was placed into the above-described cell, and the indicator electrode was inserted. At least 24 h was allowed for the gelation. After the drying and aging, during which the volume shrinks, silica monoliths with an approximate volume of 9×10^{-5} dm^{-3} were produced.

Results and discussion

Fabrication and electrochemical characterization of FeHCNFe-containing gels

As described above, the encapsulation of FeHCNFe is initiated by including Prussian Yellow, $Fe^{III}[Fe^{III}(CN)_6]$, in the sol. During the gelation and aging, a transition to a blue-green species is apparent in the optically transparent material. The color change, along with the voltammetry described below, is indicative of the formation of colloidal PB ($KFe^{III}[Fe^{II}(CN)_6]$), perhaps in combination with Berlin Green, $\{Fe^{III}[Fe^{III}(CN)_6]\}_x$ $\{KFe^{III}[Fe^{II}(CN)_6]\}_{1-x}$ ($0 < x < 1$). The reductive reorganization of Prussian Yellow to Berlin Green in the acidic environment of the sol-gel reaction is caused by the oxidization of chloride to chlorine.

Unlike the precipitate formation between the surfactant and the substrate that we found in a study on phosphotungstic acid in silica [2, 6], in the present work, chemical interaction between the FeHCNFe and the silica matrix was not observed. Atomic microscopy images (not presented here) show that when our gels were prepared from sols containing surfactant at concentrations where liquid crystals may exist, the surface of the resulting gels reflect a mesoporosity. In the absence of surfactant, the surfaces, although not ordered, suggest that the pores and interstitial spaces between the colloidal precursors are significantly smaller. Atomic force study of these gels will be the subject of a future report.

Figures 1 and 2 show cyclic voltammetric responses of FeHCNFe encapsulated in silica gel following drying at ambient conditions for 5 days. The results are consistent with the well-known voltammetry of PB in the form of films or mechanically attached particles on electrode surfaces [13, 20, 23, 24]. The system is characterized by two redox reactions: oxidation of PB to Prussian Yellow and reduction of PB to Prussian White (Everitt's Salt), $K_2Fe^{II}[Fe^{II}(CN)_6]$. Here, the latter process is of primary interest because the electrochemical oxidation of PB is more poorly defined in that it proceeds via a mixed intermediate form, Berlin Green. The electrochemical reduction of PB

$$KFe^{III}[Fe^{II}(CN)_6] + e^- + K^+ \Leftrightarrow K_2Fe^{II}[Fe^{II}(CN)_6] \quad (1)$$

is accompanied by the motion of cations, of which K^+ is considered particularly favorable. Because of the composition of the precursor solution, the silica contains a sufficient population (ionic budget) of mobile K^+ to support the redox of PB species.

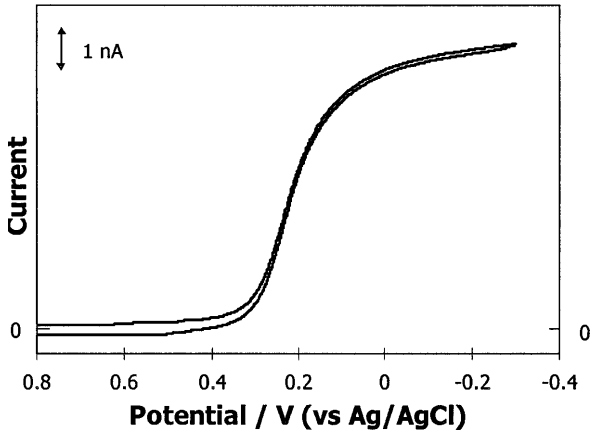

Fig. 1 Voltammetric response at slow scan rate (4 mV s^{-1}) with PB-doped silica as the solid state cell. Working electrode, carbon fiber ultramicrodisk of 10-μm diameter. The silica was aged for 120 h and used without contact to an external solution

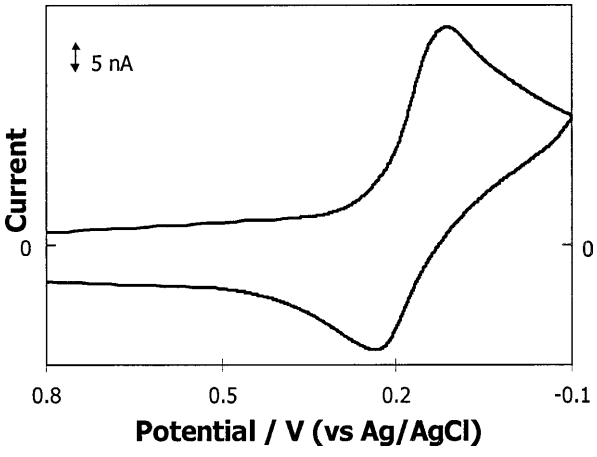

Fig. 2 Voltammetric response at a fast scan rate (50 V s^{-1}) with PB-doped silica as the solid state cell. Other parameters are those in Fig. 1

The voltammograms in Figs. 1 and 2 were recorded in two time regimes, namely a slow (4 mV s^{-1}) and a fast (50 V s^{-1}) scan rate, which yielded different diffusional behavior. The sigmoidal shape of voltammogram in Fig. 1 suggested that the operative mass transport mode was hemispherical flux of redox centers to the planar electrode with the diffusional field much larger than the size of electrode. That is, $\tau \gg 1$, where τ is the dimensionless time parameter 4 $D_{app}t/r^2$ (where D_{app} is an apparent, or effective, diffusion coefficient, t the time, and r the electrode radius) [25, 26]. On the other hand, a typical peak-shaped response (Fig. 2) was obtained in the case of a fast scan rate (i.e., short-time) experiment. This result was consistent with $\tau \ll 1$, in which case the diffusional field is small in comparison to the electrode radius, and the diffusional flux is perpendicular to the electrode surface (planar diffusion).

To test the above models of charge propagation in the PB-doped silica, the influence of scan rate, v, on the current was examined. A linear plot of i_p versus $v^{1/2}$, where i_p is the peak current, was observed in the v-range above ca. 50 mV s^{-1}, which supported the model that planar diffusion limits the current in this time domain. In this regard, it was demonstrated previously [2, 6] that the Randles-Ševcik equation

$$i_p = 2.69 \times 10^5 n^{3/2} A D_{app}{}^{1/2} C_o v^{1/2} \quad (2)$$

is applicable to xerogel matrices in the absence of a contacting liquid phase. Here, C_o, A, and n denote the concentration of redox sites, electrode surface area, and number of electrons involved, respectively. From the linearity of Fig. 3, kinetic limitations, which produce negative deviations from linearity, were not observed at fast scan rates.

Consistent with previous studies in silica electrolytes [2, 6], at sufficiently slow scan rates (below 4 mV s^{-1} in Fig. 3), voltammetric currents become independent of v. The steady-state (plateau) currents, i_{ss}, are related to the expression

$$i_{ss} = 4nFrD_{app}C_o \quad (3)$$

which is applicable to disk electrodes in a time domain where $\tau \gg 1$. Equation 3 also describes the steady-state currents in a long-pulse (30 s) chronoamperometry with working electrodes of the dimension employed herein. The i_{ss} value of the chronoamperometry experiment in Fig. 4 is indeed the same as that in voltammetry. The rapid decay of the reverse current in Fig. 4 is related to the limited quantity of electrolysis product near the working electrode when $\tau \gg 1$.

An alternative approach to the data analysis is to plot the chronocoulometric charge, Q, versus $t^{1/2}$ (Fig. 5). Monitoring Q over a short time, 10 ms, yields a linear dependence which follows the integrated form of the Cottrell equation

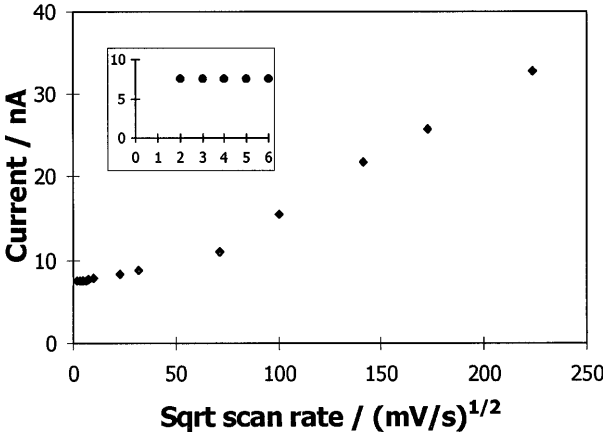

Fig. 3 Dependence of voltammetric peak (reduction) currents on the square root of the scan rate. *Inset* shows the dependence of plateau currents at the slow scan rates. The parameters other than scan rate are those in Fig. 1

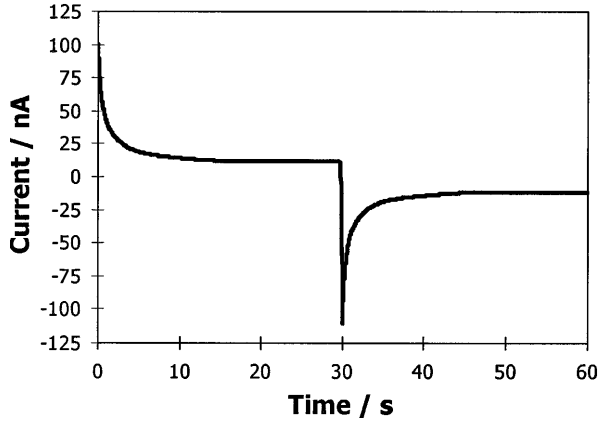

Fig. 4 Double potential step chronoamperometry of PB-doped silica. Pulse length, 30 s. The potential step was from 1.0 V to −0.4 V vs. solid Ag/AgCl. Other parameter are those in Fig. 1

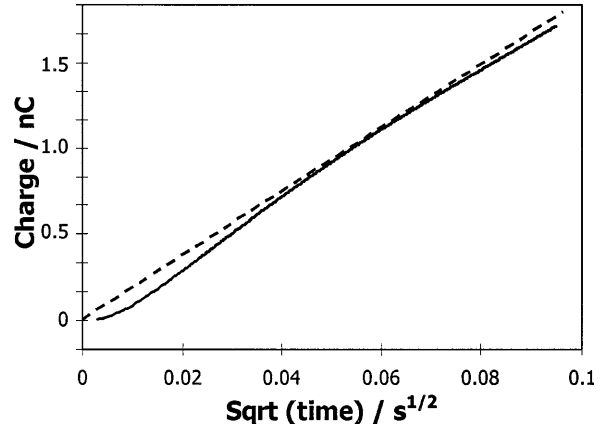

Fig. 5 Chronocoulometry of PB-doped silica. Pulse length, 0.01 s. Other parameters as for Fig. 4

$$Q = 2nFr^2\pi^{1/2}D_{app}^{1/2}C_o t^{1/2} \quad (4)$$

This behavior is evidence that planar diffusion is the limiting charge transport mechanism. In turn, the linearity suggests the absence of ohmic losses, migration effects, or slow interfacial electron transfer during the measurement [3, 26]. Recalling that $\tau = 4\ D_{app}t/r^2$, the fact that i_{ss} ($\tau \gg 1$) is developed at moderate scan rates (e.g. 4 mV s^{-1} in Fig. 3) implies that the overall dynamics of charge propagation is fast [27]. Apparently, FeHCNFe-containing silica prepared by sol-gel chemistry with drying at room temperature for 5 days retains sufficient moisture to keep K^+ hydrated and mobile.

Using a previously reported method [2, 3, 6, 26, 28], C_o and D_{app} were determined from voltammetric data. By employing scan rates of 50 V s^{-1} and 4 mV s^{-1}, currents were obtained in the short-time and long-time regimes of Fig. 3, which are described by Eqs. 2 and 3, respectively. Solution of this system of two equations in two unknowns yielded [28]:

$$D_{app} = [(2.69 \times 10^5)^2 n v \pi^2 r^2 i_{ss}^2]/(16F^2 i_p^2) \quad (5)$$

$$C_o = (4Fi_p^2)/[(2.69 \times 10^5)^2 i_{ss} v n^2 \pi^2 r^3] \quad (6)$$

When FeHCNFe-doped silica that was aged for 5 days was subjected to voltammetric analysis, the following values were obtained from Eqs. 5 and 6: $D_{app} = 2.0 \times 10^{-6}$ cm^2 s^{-1} and $C_o = 1.4 \times 10^{-2}$ mol dm^{-3}.

In an analogous manner, long-pulse chronoamperometry and short-pulse chronocoulometry were used to determine C_o and D_{app} from expressions derived previously [27] from Eqs. 3 and 4:

$$D_{app} = (i_{ss}^2 \pi r^2)/[4(Q/t^{1/2})^2] \quad (7)$$

$$C_o = (Q/t^{1/2})^2/(nF\pi r^3 i_{ss}) \quad (8)$$

Equations 7 and 8 were used for analysis of data from experiments that were performed under the conditions in Figs. 4 and 5. The following parameters were obtained: $D_{app} = 1.9 \times 10^{-6}$ cm^2 s^{-1}; $C_o = 1.4 \times 10^{-2}$ mol dm^{-3}. That these results agreed with those from voltammetry was not surprising. It was previously reported that virtually identical results were obtained from the combinations of Eqs. 5 and 6 and of Eqs. 7 and 8 if cyclic voltammetric responses are well defined and if the diffusional diagnostic criteria are met [2, 6, 29]. However, it is important to note that potential step approaches are generally more tolerant of resistive conditions [30]; therefore, they are usually more suitable for quantitative diffusion measurements in solid state electrochemistry of rigid and semirigid materials.

The general results obtained by combinations of cyclic voltammetric and of potential step experiments were confirmed by a curve-fitting procedure using the expression [2, 31]:

$$i = 4nFDrC[0.7854 + 0.8862t^{-1/2} + 0.2146\exp(-0.7823t^{-1/2})] \quad (9)$$

The data were obtained as described in Fig. 4. The values of D_{app} and C_o obtained from an 80-point plot for PB-doped silica that was aged for 120 h equal 1.8×10^{-6} cm^2 s^{-1} and 1.4×10^{-2} mol dm^{-3}, respectively.

Comparison to aqueous solution measurements

The values of D_{app} and C_o obtained in the above experiments suggests that the redox of FeHCNFe in these silica monoliths approaches a physical diffusion limit. Presumably, the electron-transfer process is controlled by diffusion in the pore volume of the silica. In this regard, the formulation that was used to prepare the monoliths yields silica with a water content of about 20% when aged for 1–5 days [6]. The high water content reflects the mesoporosity of the silica that is prepared in the presence of a concentrated surfactant. A test of this model is to perform experiments in an aqueous solution that contains a true concentration of the electroactive species which is comparable to the C_o-value obtained in

silica. If the model is valid, the resulting diffusion coefficient is predicted to be similar to the D_{app} that is measured in silica.

Aqueous solutions were prepared with iron(III) hexacyanoferrate(III) concentrations of 1.0×10^{-2} and 5.0×10^{-3} mol dm^{-3} by simply mixing equivalent amounts of $FeCl_3$ and $K_3[Fe(CN)_6]$. Solutions of concentrations higher than 1×10^{-2} mol dm^{-3} were not studied because reproducible steady-state plateau currents at slow scan rates or during long potential steps were not observed. This irreproducibility probably resulted from uncontrolled formation of FeHCNFe films on the surfaces of the ultramicrodisk working electrodes. Such a problem neither occurred during studies in silica nor in FeHCNFe solution at concentrations not exceeding 1.0×10^{-2} mol dm^{-3}. Under these conditions, the obtained data could be reproduced during prolonged or repetitive voltammetric and potential step experiments.

The voltammetric results, which are summarized in Fig. 6, were consistent with the expected transition from hemispherical flux of redox species to the electrode surface (i.e. $\tau \gg 1$) to semi-infinite linear diffusion ($\tau \ll 1$) as the scan rate is increased. In order to quantify the mass transport model, we examined the influence of $v^{1/2}$ on the reduction currents of the 1.0×10^{-2} mol dm^{-3} iron(III) hexacyanoferrate(III) solution (Fig. 6). Below 20 mV s^{-1} (see inset to Fig. 6), a steady-state limiting current, which was independent of v, was developed; i.e., hemispherical flux ($\tau \gg 1$) was the mass transport mode. At $v > 10$ V s^{-1}, voltammetric peaks rather than plateau currents were observed, which is indicative of linear diffusion ($\tau \ll 1$); consistent with linear diffusion, the peak currents were directly proportional to $v^{1/2}$. Because these limiting conditions were observed, the values of D_{app} and C_o were estimated using Eqs. 5 and 6. For the 1.0×10^{-2} mol dm^{-3} iron(III) hexacyanoferrate(III) solutions, the following values were calculated:

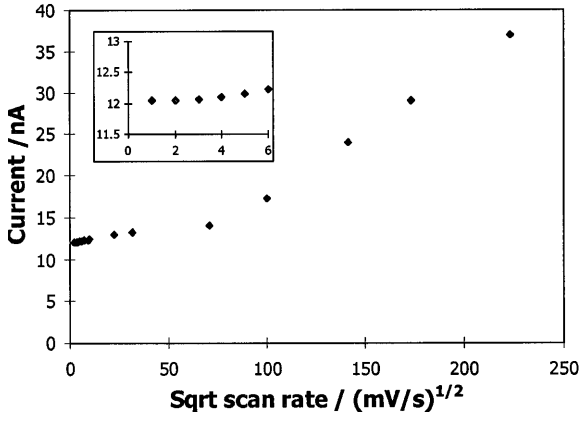

Fig. 6 Dependence of voltammetric peak (reduction) currents on the square root of the scan rate with a solution of 1.0×10^{-2} mol dm^{-3} iron(III) hexacyanoferrate(III) in 0.2 mol dm^{-3} KCl. Working electrode, carbon fiber ultramicrodisk of 10 μm diameter

$D_{app} = 5.5 \times 10^{-6}$ cm^2 s^{-1} and $C_o = 1.0 \times 10^{-2}$ mol dm^{-3}. At 5.0×10^{-3} mol dm^{-3} iron(III) hexacyanoferrate(III), the respective values obtained for D_{app} and C_o were 5.7×10^{-6} cm^2 s^{-1} and 5.1×10^{-3} mol dm^{-3}.

The determination of D_{app} and C_o in aqueous solution was repeated by potential-step experiments as described in Fig. 4. As in the case where silica was the medium, limiting conditions (at which Eqs. 7 and 8 were obeyed) were attained for 1.0×10^{-2} mol dm^{-3} iron(III) hexacyanoferrate(III) in aqueous solution. The values of D_{app} and C_o that were measured were 6.0×10^{-6} cm^2 s^{-1} and 1.0×10^{-2} mol dm^{-3}, respectively. Finally, fitting the current-time curve to the Shoup-Szabo expression [31] yielded $D_{app} = 5.2 \times 10^{-6}$ cm^2 s^{-1} and $C_o = 1.0 \times 10^{-2}$ mol dm^{-3}. Thus, the potential-step and the voltammetric methods yield mass transport parameters that agree. Of importance is that the D_{app} values in the aqueous solution experiments and those determined in silica were approximately in the same range. Apparently, the mass transport in the pore volume was comparable to that in aqueous solution. It is plausible to assume that the pore-immobilized FeHCNFe species were predominantly in a colloidal form rather than in polymeric state. This statement is in agreement with the visual examination of FeHCNFe-containing silica for which no rigid polymeric PB aggregates were observed.

Conclusions

The values of D_{app} and C_o which are obtained in the above experiments are estimates. The uncertainty of the active electrode area and the possibility of some blocking of the electrode area by the silica backbone are limiting factors. Nevertheless, the consistency of the results allows us to draw certain conclusions. First, the dynamics of charge propagation in FeHCNFe-doped xerogels are only somewhat smaller than in iron hexacyanoferrate solutions of comparable concentration. The near agreement suggests an important role of residual water existing in the pores of the silica. Similar behavior was observed previously by us for heteropolyacids of tungsten encapsulated by sol-gel chemistry. The D_{app} values can be viewed in terms of a corrected form of the Dahms-Ruff relationship [32] that describes coupling between physical diffusion (D_{phys}) and electron hopping (self-exchange) to produce the net or apparent diffusivity, termed D_{app} herein:

$$D_{app} = D_{phys} + k_{ex}\delta^2 C_o/6 \quad (10)$$

where k_{ex} is a self exchange rate, and δ is an average center-to-center distance between the iron hexacyanoferrate units in the gel. Where C_o is 0.01 mol dm^{-3}, the contribution to D_{app} from self-exchange is relatively small even when k_{ex} is high. Further, the values of D_{app} that are estimated in the aqueous solution experiments, ca. 6×10^{-6} cm^2 s^{-1}, and in the gel, ca. 2×10^{-6} cm^2 s^{-1}, are comparable, and they are

much larger than D_{app} reported for solid (polymeric) PB, ca. 10^{-9} cm^2 s^{-1} [27, 33]. Hence, it is plausible to assume that, from a mechanistic viewpoint, mass transport is predominantly from physical diffusion of dispersed, colloidal, FeHCNFe species. During voltammetric measurements utilizing ultramicroelectrodes, only a small fraction of redox centers is electrolyzed and, consequently, formation of rigid polymeric PB agglomerates is minimized.

Acknowledgements This work was supported by the National Science Foundation through grant INT-9529589 and by the State Committee for Scientific Research (KBN), Poland, under grant 3T09A 09313. A travel grant from the Batory Foundation was provided to K.M.

References

1. Oliver BN, Coury LA, Egekeze JO, Sosnoff CS, Zhang Y, Murray RW, Keller C, Umana MX (1990) In: Buck RP, Hatfield WE, Umana MX, Bowden EF (eds) Biosensor Technology: Fundamentals and Applications, Chap 8. Dekker, New York
2. Cox JA, Wolkiewicz AM, Kulesza PJ (1998) J Solid State Electrochem 2: 247
3. Kulesza PJ, Cox JA (1998) Electroanalysis 10: 73
4. Meixner DL, Gilicinski AG, Dyer PN (1998) Langmuir 14: 3202
5. Lev O, Wu Z, Bharathi S, Glezer V, Modestov A, Gun J, Rabinovich L, Sampath S (1997) Chem Mater 9: 2354
6. Holmstrom SD, Karwowska B, Cox JA, Kulesza PJ (1998) J Electroanal Chem 456: 239
7. Audebert P, Griesmar P, Sanchez C (1991) J Mater Chem 1: 699
8. Makote R, Collinson MM (1998) Chem Mater 10: 2440
9. Lee M-H, Kim Y-T (1999) Electrochem Solid-State Lett 2: 72
10. Pyo M, Bard AJ (1997) Electrochim Acta 42: 3077
11. Tanev PT, Pinnavaia TJ (1995) Science 267: 865
12. Alber KS, Cox JA (1997) Mikrochim Acta 127: 131
13. Feldman BJ, Murray RW (1987) Inorg Chem 26: 1702
14. Kulesza PJ (1990) Inorg Chem 29: 2395
15. Carpenter MK, Connel RS, Simko SJ (1990) Inorg Chem 29: 845
16. Kulesza PJ, Malik MA, Berrettoni M, Giorgetti M, Zamponi S, Schmidt R, Marassi R (1998) J Phys Chem B 102: 1870
17. Coon DR, Amos LJ, Bocarsly AB, Fitzgerald PA Bocarsly (1998) Anal Chem 70: 3137
18. Dussel H, Dostal A, Scholz F (1996) Fresenius J Anal Chem 355: 21
19. Malik MA, Horanyi G, Kulesza PJ, Inzelt G, Kertesz V, Schmidt R, Czirok E (1998) J Electroanal Chem 452: 57
20. Neff VD (1985) J Electrochem Soc 132: 1382
21. Kahn O (1995) Nature 378: 667
22. Ohkoshi S, Fujishima A, Hashimoto K (1998) J Am Chem Soc 120: 5349
23. Kulesza PJ, Doblehofer K (1989) J Electroanal Chem 274: 95
24. Dostal A, Meyer B, Scholtz F, Schroder U, Bond MA, Marken F, Shaw SJ (1995) J Phys Chem 99: 2096
25. Wightman RM, Wipf DO (1989) In: Bard AJ (ed) Electroanalytical chemistry, vol 15. Dekker, New York, pp 268–353
26. Aoki K, Osteryoung J (1984) J Electroanal Chem 160: 335
27. Kulesza PJ, Faulkner LR (1993) J Am Chem Soc 115: 11878
28. Kulesza PJ, Chelmecki G, Galadyk B (1993) J Electroanal Chem 347: 417
29. Kulesza PJ, Karwowska B, Malik MA (1998) Colloids Surf A 134: 173
30. Haas O, Valazquez CS, Porat Z, Murray RW (1995) J Phys Chem 99: 15279
31. Shoup DJ, Szabo A (1982) J Electroanal Chem 140: 237
32. Majda M (1992) In: Murray RW (ed) Molecular design of electrode surfaces. Wiley, New York
33. Kulesza PJ (1990) J Electroanal Chem 289: 103